

4-3-1993

## Electron Beam Induced Current Studies of Defect Induced Conductivity Inversion

Z. J. Radzimski

*North Carolina State University*

A. Buczkowski

*North Carolina State University*

T. Q. Zhou

*North Carolina State University*

C. Dubé

*Mobil Solar Research Corporation*

G. A. Rozgonyi

*North Carolina State University*

Follow this and additional works at: <https://digitalcommons.usu.edu/microscopy>

 Part of the [Biology Commons](#)

---

### Recommended Citation

Radzimski, Z. J.; Buczkowski, A.; Zhou, T. Q.; Dubé, C.; and Rozgonyi, G. A. (1993) "Electron Beam Induced Current Studies of Defect Induced Conductivity Inversion," *Scanning Microscopy*: Vol. 7 : No. 2 , Article 7. Available at: <https://digitalcommons.usu.edu/microscopy/vol7/iss2/7>

This Article is brought to you for free and open access by the Western Dairy Center at DigitalCommons@USU. It has been accepted for inclusion in Scanning Microscopy by an authorized administrator of DigitalCommons@USU. For more information, please contact [digitalcommons@usu.edu](mailto:digitalcommons@usu.edu).

## ELECTRON BEAM INDUCED CURRENT STUDIES OF DEFECT INDUCED CONDUCTIVITY INVERSION

Z. J. Radzimski\*, A. Buczkowski<sup>1</sup>), T.Q. Zhou<sup>1</sup>), C. Dubé<sup>2</sup>) and G. A. Rozgonyi<sup>1</sup>)

Analytical Instrumentation Facility

<sup>1</sup>)Department of Materials Science and Engineering

North Carolina State University, Raleigh, NC 27695-7916

<sup>2</sup>)Mobil Solar Research Corporation, Billerica, MA 01821-3980

(Received for publication August 13, 1992, and in revised form April 3, 1993)

### Abstract

Defect induced inversion of conductivity type was studied both at the surface and at a network of interfacially confined misfit dislocations in heteroepitaxial Si(Ge) on Si structures. The inversion was achieved by controlled contamination with Au and Ni metallic impurities introduced by diffusion from backside evaporated layers. A theoretical explanation of the defect electrical activity and the inversion effect is presented, along with temperature dependent beam induced current observations.

### Introduction

Electrically active defects influence the properties of semiconductors in a variety of ways [6,12,13,15]. The impact of the defect on a particular material or device property will scale with the defect "strength", density and distribution. Deep energy level defects, being strong recombination centers, are considered to be prime lifetime killers. Shallow defects are less active at room temperature, but their activity increases strongly when the temperature is decreased [1,10,14]. In the case of isolated extended defects, local perturbations of the semiconductor electrical properties occur which give rise to the formation of local internal electric fields. For a high density of defects distributed relatively uniformly their electrically active volumes overlap, and the entire semiconductor volume is modified. Thus, above a certain threshold value of defect density, an inversion of conductivity type may occur. Inversion associated with a defect or group of defects is particularly important for one or two dimensional device structures, such as conducting wires or buried junctions, for which the defect is an active part of an electron device. In this report, we examine this defect induced inversion, using the electron beam induced current (EBIC) technique in a scanning electron microscope (SEM) and present a phenomenological explanation of the effect.

### Inversion Phenomena - Theoretical Approach

The impact of structural defects and impurities on the properties of the surrounding semiconductor material can be analyzed theoretically by calculation of the potential distribution induced by trap charges. In the case of impurities gettered at the surface, a surface potential induced by a trap associated with contaminants would be considered. In the case of an interfacial misfit dislocation plane, it would be the potential of this plane induced by a trap charge associated with dislocations or dislocation/impurity complexes. The charge depends on the trap concentration, their donor or acceptor type nature, the occupancy status, and its temperature dependence. For example, for acceptor type states the charge is neutral when these states are empty and negative when filled with electrons. Based on the equations given by Many et al. [9], the surface potential change or the concentration of free carriers due to the trap presence can be calculated from the neutrality requirement

**Key words:** Electron beam induced current, defect electrical activity, impurity gettering, misfit dislocations, heteroepitaxy.

\* Address for correspondence:

Zbigniew J. Radzimski

Analytical Instrumentation Facility, North Carolina State University, Raleigh, NC 27695-7916

Phone No. (919) 515 - 7622

for surface and space charge region charges. The theoretical results are given in Fig. 1a for n-type material with acceptor type states of 0 eV energy as an example. Note that the reference (zero) energy level is assigned to the mid-gap intrinsic energy level  $E_i$ . As the concentration of acceptor traps increases, the concentration of holes also increases. A significant increase of holes for 0 eV traps occurs between  $10^{10}$  and  $10^{11}/\text{cm}^2$  surface concentration. The point where the concentration of holes provided by surface is equal to the intrinsic concentration of electrons defines the critical value of trap density  $N_{Tcr}$  which induces conductivity type inversion. When donor type states are considered to be present at the surface, then an  $n^+$  region is formed. For donor traps with energy +0.3eV, this effect is noticeable when the surface concentration is higher than  $10^9/\text{cm}^2$ , as shown in Fig. 1b.

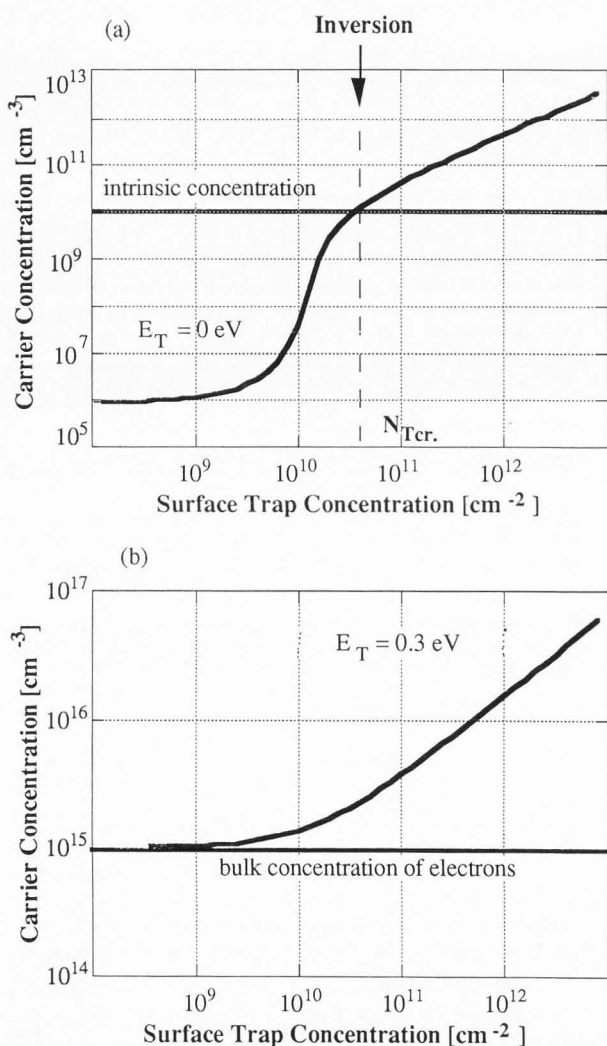


Fig. 1. Surface concentration of (a) holes for acceptor type traps located at  $E_T = 0 \text{ eV}$ , and (b) electrons for donor traps at  $E_T = 0.3 \text{ eV}$ , as a function of trap density in n-type silicon. Intrinsic and bulk electron concentration levels, in (a) and (b) respectively, are also shown as a reference. Calculations were done for room temperature.

The critical value of trap density for conductivity type inversion to occur depends strongly on trap energy and sample temperature. This is shown in Fig. 2 for acceptor traps with various energy levels in n-type material. As the sample temperature decreases the probability for a trap to provide a carrier decreases, thus more traps are needed to change the conductivity type. The probability also decreases when the trap energy increases.

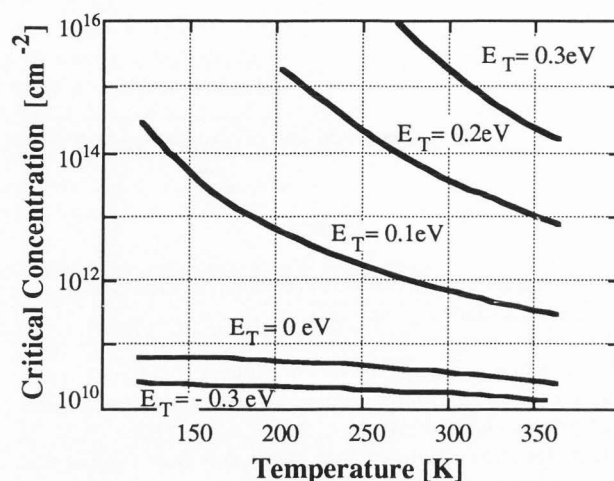


Fig. 2. Temperature dependence of the critical surface concentration of acceptor traps with various energies for which conductivity inversion occurs in n-type Si. Background donor concentration =  $1 \times 10^{14} \text{ cm}^{-3}$ .

### Experiment

Defect induced conductivity inversion was studied both at the surface and at a network of interfacially confined misfit dislocations in heteroepitaxial Si(Ge) structures. The dislocations were intentionally introduced by adding small amounts of Ge (1% to 2%) during CVD Si epitaxial growth at  $1120^\circ\text{C}$  [15]. In this way, two interfacial planes of dislocations are formed between the buried Si(Ge) layer and a Si capping layer and Si substrate. The depth of the buried misfit dislocations can be defined precisely by adjusting the thickness of the pure Si capping layer. Dislocation density can be controlled by adjusting the Ge content in the Si(Ge) layer. Such dislocations are thermally stable due to their large free energy of formation and the small diffusivity of Ge in Si. The dislocations were subsequently decorated with various metallic impurities by diffusion from a backside evaporated layer during rapid thermal annealing at temperature from  $400^\circ\text{C}$  to  $1130^\circ\text{C}$  for 30 seconds. It has been shown that a wide spectrum of Au and Ni decoration can be achieved during this short annealing time, ranging from light decoration up to the formation of large precipitates. During diffusion at temperatures higher than  $800^\circ\text{C}$ , some of the impurities pass through the interfacial misfit dislocation planes and are gettered at the top surface. This has been confirmed earlier by RBS analysis and TEM observation [18,19]. These impurities alter the electrical properties of the surface to the point where a conductivity inversion occurs.

### EBIC Characterization of Defects

The EBIC technique is a well recognized method for characterizing the electrical activity of semiconductor material and defects [3-5,11]. The EBIC signal depends on carrier diffusion length and internal electrical field. Any local variation of these properties is a source for EBIC contrast. A typical EBIC image of a Schottky contact fabricated on the semiconductor with uniform bulk properties shows a bright area at the contact and a dark area outside the contact. The bright area corresponds to the region where carriers generated by the electron beam are separated by the electric field of the Schottky contact and collected by this contact giving rise to the external circuit current. On other hand, if no electric field exists, the electron-hole pairs generated by electron beam recombine, no current is collected, and a dark region is observed. The same bright/ dark contrast convention is used for Schottky contacts on either n- or p-type substrates, even though a positive (negative) potential is always generated on p - type (n - type) material. Examples of EBIC images for Si(Ge) n-type samples are given in Figs. 3a and b, where dislocations decorated with gold and nickel at 1000°C for 30 seconds can be seen. The bright 1mm diam Schottky contacts are clearly visible in these images with dark lines corresponding to electrically active misfit dislocations. The differences in electrical activity of Au and Ni decorated misfit dislocations depend on the level and the morphology of decoration. For example, Au precipitates in a

high density of closely spaced ( $<1 \mu\text{m}$ ) colonies, while Ni forms large  $\text{NiSi}_2$  precipitates separated by 5 to 20  $\mu\text{m}$ . Additional discussion on this subject can be found in Refs. [13,14,18].

### Experimental Results

#### Surface inversion

Defect activation during rapid thermal annealing results in an increased EBIC contrast of buried misfit dislocations reflecting their increased electrical activity due to impurity gettering. However, after annealing at temperature 1000°C and below no change in the EBIC electrical activity of the top surface layer of the investigated samples was observed. This indicates that the amount of impurity that diffuses past the buried misfit interface was too small to alter the electrical properties of the surface layer. This corresponds to the flat portion of the curves in Fig. 1a and b where the influence of surface traps on background concentration of majority carriers is negligible. However, as the impurity level increases following an 1130°C annealing, an unexpectedly strong EBIC signal is collected far beyond the 1 mm diameter Schottky contact for both Ni and Au decorated samples, as shown in Figs. 4a and b. The signal collected beyond the contact area can only arise from a built-in electric field which separates carries in a fashion similar to the electric field of a Schottky contact. The

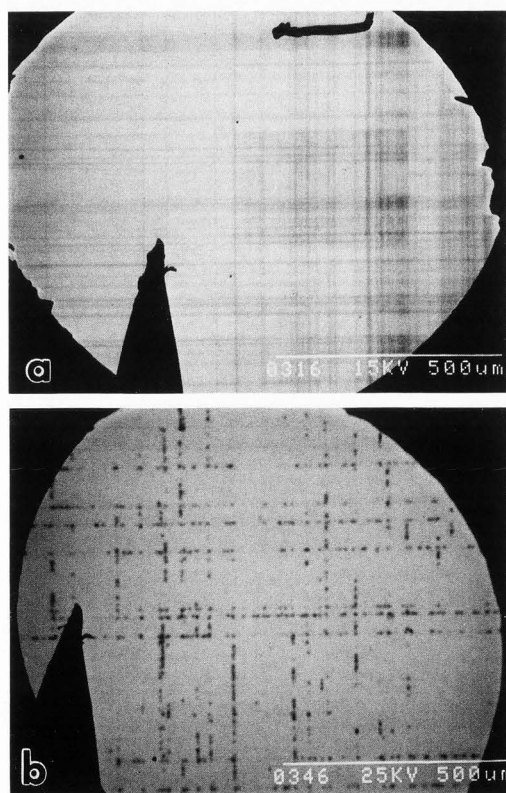


Fig. 3. EBIC/SEM image of Si(Ge) heterostructures with misfit dislocations following decoration with (a) Au and (b) Ni at 1000°C for 30 sec.

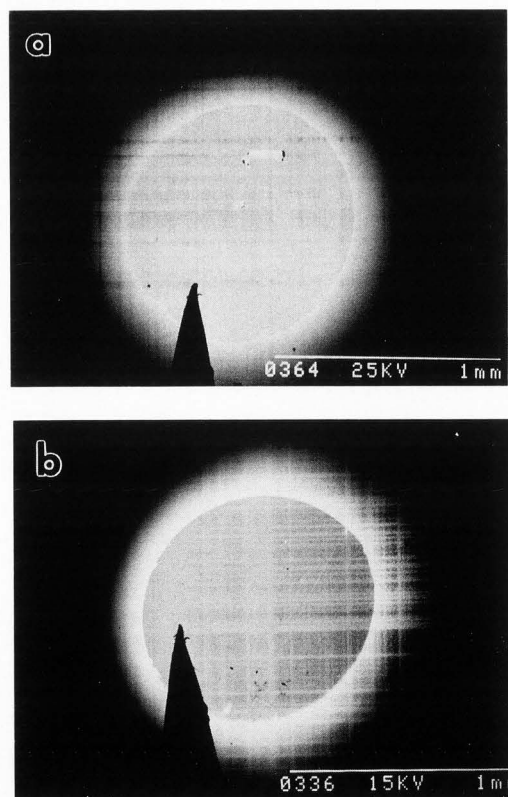


Fig. 4. EBIC/SEM image of the misfit dislocation heterostructure following decoration with (a) Au and (b) Ni at 1130°C for 30 sec.

presence of this unexpected electric field was only found in samples subjected to a high temperature decoration process. Note also that the buried misfit dislocations appear as dark lines in all Au diffused samples; whereas they are white or dark in the Ni sample annealed at high or moderate temperatures, respectively. This effect of contrast inversion will be discussed in more detail below.

To define the depth over which the extended lateral electric field acts, angle polished samples were prepared such that the Schottky contact simultaneously overlapped the top surface layer and the various "buried" interfaces. Close examination of the EBIC image of the beveled Au decorated sample, see Fig. 5, indicates that the extended contrast observed on the top surface (region "C") is confined to a shallow layer near the top surface where a conductivity inversion, from the original n-type to p-type, occurred. This is accompanied by a contrast change from black (where no collection was present in samples annealed at lower temperatures) to white, representative of p-type material. Thus, the outlined Au contact (region "B"), which overlaps both the top and angle polished surfaces, functions as an ohmic contact to the inverted surface layer.

A similar observation regarding the occurrence of a surface inversion layer was revealed in the Ni sample, see Fig. 6, where the contrast abruptly ends on the bevelled surface at the edge of the Schottky contact, but extends far beyond the contact on the top surface. The bevelled part of the Schottky contact on

the Ni sample also gives much higher signal than the top surface. It is important to mention that the surface inversion was not observable on Au and Ni samples annealed at or below 1000°C, for which the level of impurity decoration was below the threshold value required for surface inversion to occur.

#### Surface inversion as a function of temperature

Additional observations of the surface inversion phenomena were made by comparing EBIC images taken at different temperatures. The room temperature EBIC image in Fig. 7a shows extended area white contrast similar to that in Fig. 4a with the Au metallization acting as an ohmic contact to this layer. The contact is darker than the surrounding area because the primary electrons lose part of their energy in the metal layer reducing that available for electron-hole generation in the semiconductor. The black rectangular shape in Fig. 7a is a brass contact probe. The energy of primary electrons is completely lost in the brass probe, so the only current collected from this area is an absorbed current. This current is usually three orders of magnitude smaller than the EBIC current from an active area. Therefore, three current collection (contrast) levels corresponding to: i) the active area outside the contact, ii) the area within the contact and iii) the brass probe current can be distinguish and are shown schematically in Fig. 7b. When the

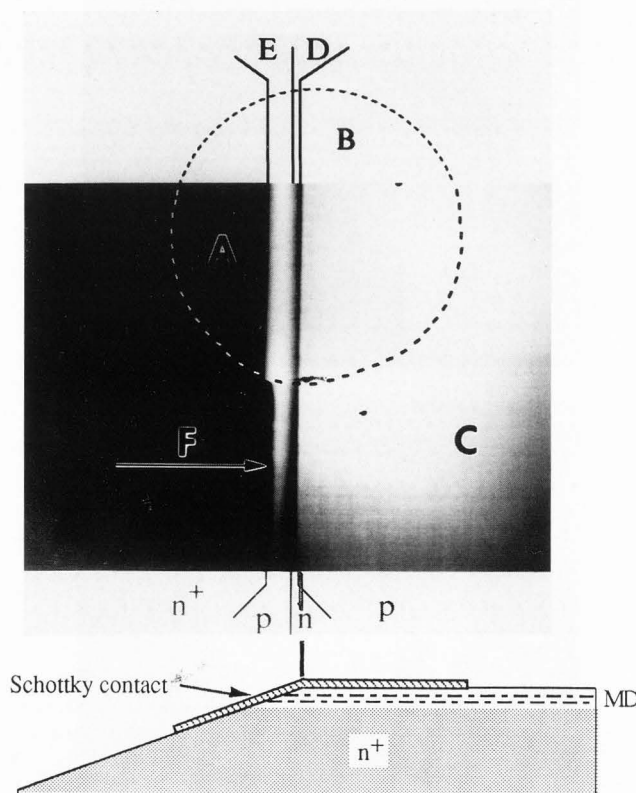


Fig. 5. EBIC/SEM image of an angle polished Si(Ge) sample decorated with Au at 1130°C (dotted line represents contour of the 1 mm diam Au Schottky contact).

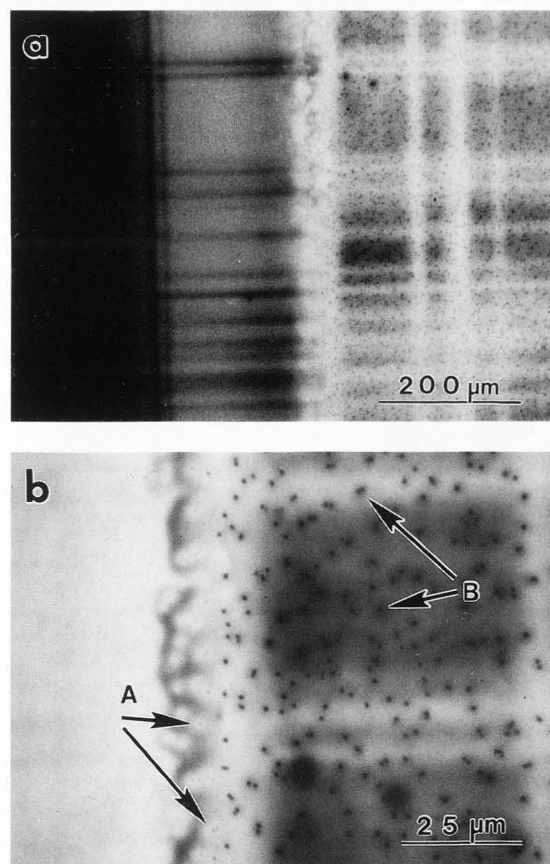


Fig. 6. EBIC/SEM images of an angle polished Si(Ge) sample decorated with Ni at 1130°C (a) low magnification and (b) high magnification of the bevelled edge area.

## EBIC of Defect Induced Conductivity Inversion

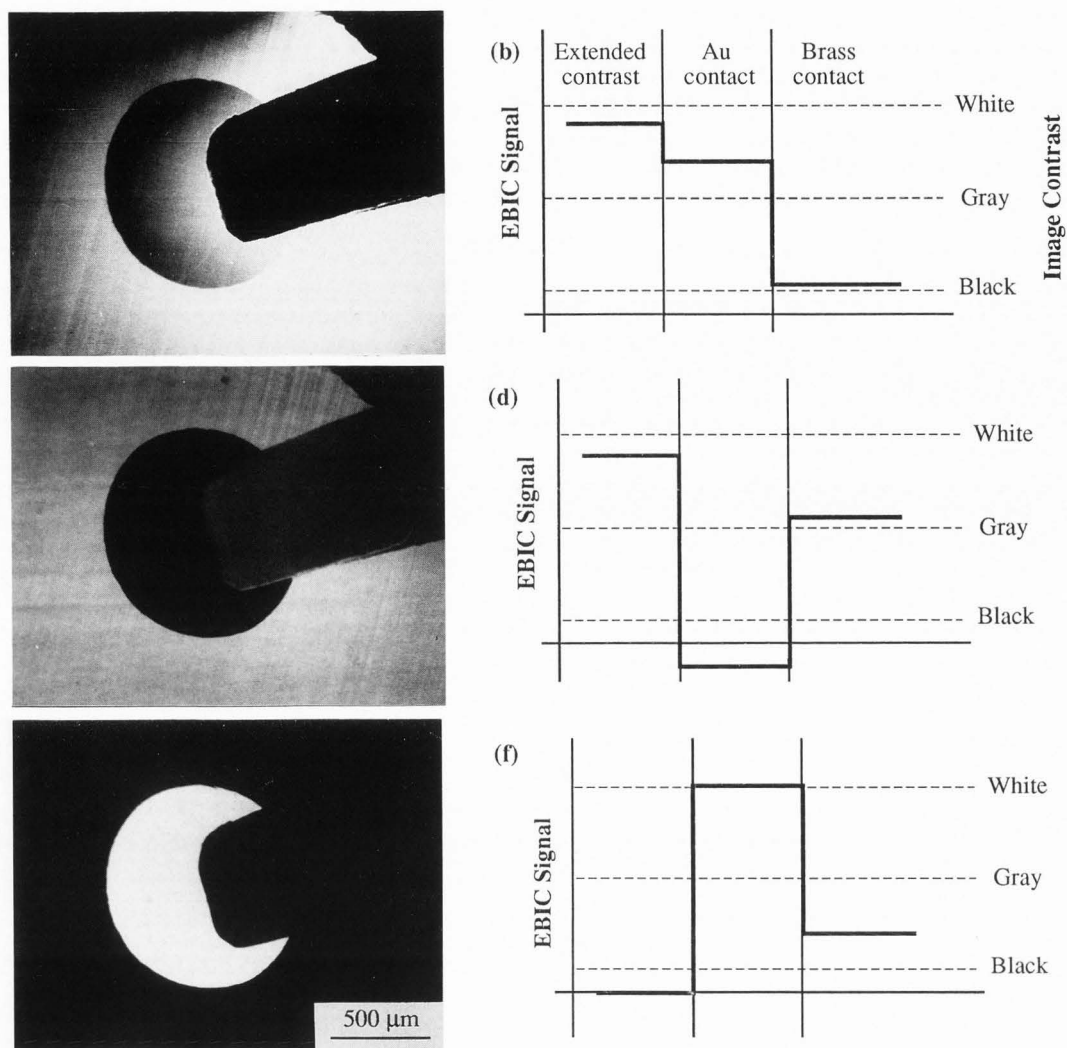


Fig. 7. EBIC/SEM image of Au decorated sample from Fig. 2a taken at (a) room temperature, (c) 130K and (e) 130K with amplifier polarity opposite to (c). The frames (b), (d) and (f) show relative signal levels corresponding to the area outside Au contact, within Au contact, and on thick brass probe.

temperature is decreased to 130K, compare Fig. 7a with 7c, the contrast outside the Au contact is approximately the same as in Fig. 7a. However, the Au contact contrast is very black, while the brass probe exhibits an intermediate or grey level of contrast, as outlined in Fig. 7d. The fact the the signal level is higher for the brass probe than for the Au contact, i.e. opposite to the room temperature image, indicates that the signal polarity changed when the temperature was decreased. Finally, switching the polarity of the EBIC amplifier of the 130 K sample results in the image shown in Fig. 7e, which is a typical EBIC image with bright contact area, as discussed earlier in this work. The signal levels for this image are shown in Fig. 7f. Summarizing these observations, the EBIC contrast at 130 K is opposite to that obtained at 300 K. In order to represent the 130 K image according to the convention used in this paper (i.e. white image indicates EBIC signal collected, dark no signal) the amplifier polarity had to be changed. When this was done, the

image contrast appeared to be the same as in the non-annealed samples or annealed at low temperatures, i.e. the EBIC current was collected only from the Schottky area. This indicates that there is no conductivity inversion at 130 K. It is important to add that the inversion effect is reversible, i.e. it returns when temperature is increased to 300 K.

### Inversion at dislocations

The near-surface conductivity inversion effect, discussed above for the Au decorated sample, is also observed at the buried misfit dislocation plane for the same sample. This additional inversion is evident in the EBIC image of the angle polished sample, see Fig. 5, where a dark band labeled "D" separates a white band "E" from the bright surface layer "B". This "D" band, whose contrast is opposite to the neighboring p - type region, must be n - type considering the polarity of the EBIC amplifier and the contrast convention adapted in this work. Moreover, the band "E" extends far beyond the perimeter

of the Schottky contact (see arrow "F"). This extended contrast is associated with the buried plane of Au-decorated misfit dislocations and indicates the presence of a buried space charge region; or in other words, the presence of an additional region with p-type properties. The band "E" was not observed in samples annealed at 1000°C and lower temperatures.

### Discussion

#### Au decorated sample

As shown theoretically in Fig. 1, there is a threshold value of defect or trap density at which an inversion of conductivity type occurs. This value depends on the energy level of the trap occupied by a structural defect, impurity or defect/impurity complex, as well as the temperature of the sample. EBIC images of Si(Ge) heteroepitaxial structures showed that such a threshold was reached both at the surface and at the misfit dislocation plane in the structure contaminated by gold and annealed at 1130°C. Two additional electric fields were detected in this structure in comparison with the samples annealed at lower temperatures, one at the surface of the epilayer and a second surrounding the core of the buried dislocation planes. A schematic illustration of these induced electric fields for the Au structure is shown in Fig. 8a. These additional electric fields are correlated with regions known to have enhanced concentration of gold (due to gettering at the surface and the dislocations) and indicate the acceptor type action of the Au contaminants. This was also confirmed by EBIC study of surface inversion as a function of sample temperature where the inversion contrast disappeared when the temperature was lowered to 130K. As shown in Fig. 2, the threshold level at which inversion occurs varies with temperature. For example, only  $8 \times 10^{11}/\text{cm}^2$  acceptor traps with energy level 0.1 eV (a typical level for gold) are required to invert the conductivity of n-type silicon with concentration  $1 \times 10^{14}/\text{cm}^3$  at room temperature. However, the inversion will not occur if the temperature is decreased to 135 K, where  $3 \times 10^{14}/\text{cm}^2$  traps are required.

#### Ni decorated sample

Surface inversion was also observed in the Ni decorated sample annealed at 1130°C, but no inversion was present around misfit dislocations. Note, however, that the dislocations in Fig. 4b are seen as white lines in the Ni sample, opposite to the Au sample, indicating that a more complicated mechanism is responsible for surface inversion in the Ni sample. Generally, defects act as recombination centers and the EBIC signal decreases locally giving rise to dark lines or spots. In this case, a defect enhancement of the EBIC signal (bright contrast) is observed. Prior observations of this effect have given rise to several reasons to explain the bright contrast [15-17]. The first one is that a local improvement of diffusion length occurs via gettering of impurities at the extended defects. In this case, the EBIC contrast shows a dark spot or line at the core of the defect surrounded by a bright zone corresponding to the improved region of semiconductor. Another reason proposed for bright contrast is the creation of a built-in electric field around the defect which attracts minority carriers. As a result, an additional charge collection takes place at the defect. The detection of this signal component, however, requires a contact

to the defect space charge region by a metal electrode to facilitate current flow in the EBIC experiment. Unfortunately, neither of these explanations can be applied to describe the white dislocation contrast.

Further EBIC work on the Ni decorated sample shown in Fig. 4b was done following angle polishing, see Fig. 6. Note that different segments of the same dislocation appear white on the top surface and dark on the bevelled part of the sample. The dark defect contrast on the bevelled surface means that the dislocation is behaving as a classical recombination site. In previous reports [13,14], we suggested that defects associated with Ni precipitates at misfit dislocations occupy deep levels and are responsible for dark EBIC contrast. Therefore, the difference in contrast (white vs. black) between the top and bevelled surfaces is not attributed to the inherent electrical activity of dislocations, but arises from different conditions of observations (potential configuration). It is important to reiterate that the dislocation contrast was the same for top and bevelled surface of the Au sample. Thus, we concluded that the top surface of the Ni sample must have a negative, i.e. reversed polarity during observation while the surface of the Au sample

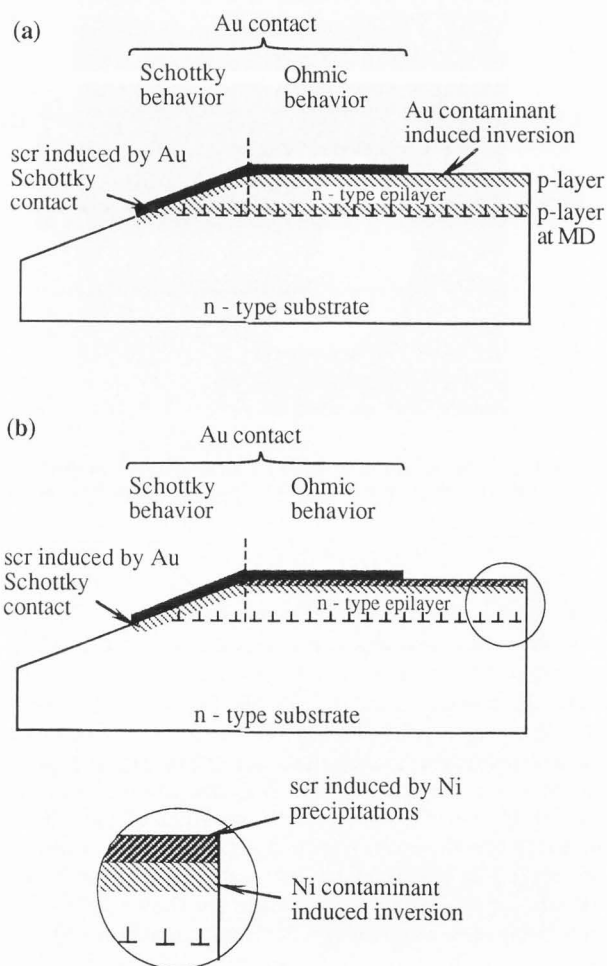


Fig. 8. Schematic representation of (a) Au, and (b) Ni decorated samples showing impurity induced inversion effects.

is positively charged. It is believed that the presence of discrete surface precipitates which populate the Ni sample, see Fig. 6, but not the Au sample, is responsible for these differences. We propose that these Ni precipitates form an additional Schottky type contact to the near-surface p-type layer which results from a uniform concentration of acceptor type defects and/or metal impurities [2] introduced during RTA annealing. The existence of such a p-type layer was confirmed by spreading resistance measurements [19]. The conductivity and polarity configuration of the top surface which was inferred from the EBIC contrast indicate that the entire top surface of the Ni sample should have a negative polarity. Cross-sectional TEM examination of the Ni precipitates indicates that they are large, approximately 1  $\mu\text{m}$  wide and 0.5  $\mu\text{m}$  deep,  $\text{NiSi}_2$  pyramids. Each of these pyramids makes a Schottky type contact creating a localized space charge region in the underlying silicon [6]. If the density of precipitates is high enough, then their space charge regions can overlap and form a continuous layer of the surface electric field, as schematically shown in Fig. 8b. This continuous near-surface layer would have a negative potential, i.e. opposite to that of the bevelled surface. Although the  $\text{NiSi}_2$  precipitates also exist in samples annealed at lower temperatures, their density and size is much lower. In this case, there is no overlap of their electric fields.

The localized space charge region around each precipitate creates a "halo" effect which is highlighted by the arrows A and B in Fig. 6b. Interesting observations can be made by comparing regions around precipitates on the top surface, arrows B with those at the upper part of the bevelled surface, see arrow A. The space charge regions surrounding the black precipitate core on the top surface are dark (grey), while on the bevelled surface they are white with a dark spot in the middle. The black precipitate core indicates strong absorption of electron beam energy in the  $\text{NiSi}_2$  silicide itself. A schematic illustration of the electric field configuration is shown in Fig. 9 for precipitates situated either on the top or on the bevelled surface. Most of an individually located precipitate resides in the p-type layer which, as suggested before, is formed by Ni atoms or other contaminants introduced during high temperature annealing. As a result, this precipitate will have a negative potential and its space charge region should be visible as a dark EBIC image. On the other hand the precipitate on the bevelled surface is situated mostly in the n-type, capping epi-layer, which should yield an opposite, i.e. white, contrast, which is confirmed in Fig. 6b.

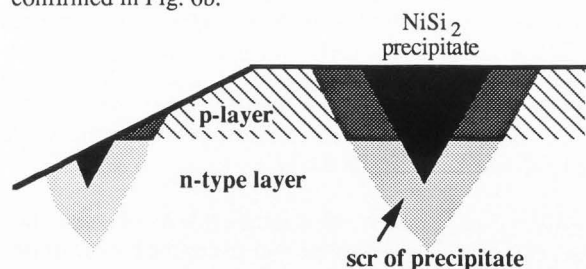


Fig. 9. Schematic representation of space charge region (scr) configuration around  $\text{NiSi}_2$  precipitates in the Ni decorated sample annealed at high temperature.

## Conclusions

It has been shown that an inversion of conductivity type may occur when the density of defects is higher than a threshold value, even if these defects are known to occupy deep levels in the band gap. This value is different for various trap levels and strongly depends on the sample temperature. The inversion of a surface layer from the original n-type to p-type was observed in the high temperature annealed Au sample. The inversion was also observed in the same sample at a misfit dislocation plane buried 4  $\mu\text{m}$  underneath a capping n-type layer. This is because Au gettering at the top surface and at the dislocations forms acceptor type traps in n-type silicon. The inversion in Ni decorated sample was observed only at the top surface layer, and is believed to be caused by a uniform distribution of Ni atoms and/or contaminants introduced during high temperature annealing. In addition, the surface  $\text{NiSi}_2$  precipitates form a sequence of Schottky contacts to this p-type layer which change the surface potential back to the negative. Thus, the near-surface electrical field configuration of Au and Ni decorated samples is opposite what results in black (Au) versus white (Ni) EBIC contrast of misfit dislocations.

## Acknowledgements

Special thanks to Jon Rossi and Don Finn at MEMC for providing Si(Ge) epitaxial substrates. This work was supported in part by MEMC, NREL, and General Instrument, Inc.

## References

1. Buczkowski A, Radzinski Z J, Kirino Y, Shimura F, Rozgonyi G A (1990) Temperature dependent recombination lifetime in silicon: Influence of trap level. Eds. P. Bristowe et al. MRS Symposium Proc. **209**, 567-572 (1991 Materials Research Society, Pittsburgh).
2. Chiavarotti G P, Conti M, Messina A (1977) Characterization of Properties of Nickel in Silicon Using Thermally Stimulated Capacitance Method, Solid-State Electronics **20**, 907-909.
3. Dimitriadis C H (1983) Carrier Recombination at Dislocations In Epitaxial Gallium Phosphide Layers, Solid-State Electronics, vol.26, pgs. 633-637.
4. Donolato C (1983) Theory of beam induced current characterization of grain boundaries in polycrystalline solar cells. Phys. Stat. Sol. (a) **54**, 1314-1322.
5. Jakubowicz A (1985) On the theory of electron-beam-induced current contrast from pointlike defects in semiconductors. J. Appl. Phys. **57**, 1194-1199.
6. Kittler M. (1989) Charge Collection Microscopy in Gettering and Defect Engineering. Solid State Phenomena **6 & 7**, 367-382.
7. Kittler M, Lärz J, Seifert W, Seibt M, Schröter W (1991) Recombination properties of structurally well defined  $\text{NiSi}_2$  precipitates in silicon. Appl. Phys. Lett. **58**, 911-913.
8. Kittler M, W. Seifert (1992) On the origin of electron beam induced current contrast of extended defects in silicon, Scanning Microscopy, **6**, 979-991.



9. Many A, Goldstein Y, Grover N B *Semiconductor Surfaces*, North-Holland Publishing Company, Amsterdam, 128-164, (1965).
10. Ourmazd A, Booker G (1979) The Electrical Recombination Efficiency of Individual Edge Dislocations and Stacking Fault Defects in n-Type Silicon. *Phys. Stat. Sol. (a)* **55**, 771-784.
11. Pearton, Corbett J W, Shi T S, (1987) Hydrogen in Crystalline Silicon. *Appl. Phys.* **A43**, 153-195
12. Radzimski Z J, Buczkowski A, Rozgonyi G A (1990) Dislocations in Heterostructures: Structural and Electrical Diagnostics. Proc. of the 12th State of Art Program on Semicond. (SOTAPOCS XII), eds. D.C.D'Avanzo, R.E. Enstrom, A.T. Macrander, D. DeCoster, ECS Proc. Vol. 90-15, 436-449.
13. Radzimski Z J, Zhou T Q, Buczkowski A, Rozgonyi G. A (1991) Electrical activity of dislocations: Prospect for practical utilization. *Appl. Phys.* **A53**, 189-193.
14. Radzimski Z J, Zhou T Q, Buczkowski A, Rozgonyi G. A, Finn D, Hellwig L G Ross J A (1992) *Appl. Phys. Lett.* **60**, 1096-1099.
15. Rozgonyi G A, Salih A S M, Radzimski Z J, Kola R R, Honeycutt J (1987) Defect engineering for VLSI epitaxial silicon. *J. of Crystal Growth*, **85**, 300-307.
16. Tung R T, Ng K K, Gibson J M, Levi A F J (1986) Schottky-barrier heights of single-crystal NiSi<sub>2</sub> on Si(111): The Effect of a surface p-n junction. *Phys. Rev. B*, **33**, 7077-7090.
17. Wilshaw P R, Fell T. (1989) The electronic properties of dislocations in silicon. *Int. Symp. on Struct. Prop. Disloc. Semicond. Oxford 1989. Inst. Phys. Conf. Ser. No. 104*, 8596-91
18. Zhou T, Buczkowski A, Radzimski Z J, Rozgonyi G A Sopori B (1991) The gettering and electrical activities of metallic impurities in epitaxial Si/Si(Ge) during rapid thermal annealing. in *Rapid thermal and Integrated Proces.* Eds. Gelpy J, Green M, Wortman J and Singh R, *MRS Proc.* **224**, 55, (MRS, Pittsburgh, PA, 1991),
19. Zhou T, Buczkowski A, Radzimski Z J, Rozgonyi G A, (1993) *J. Appl. Phys.* **73**.

### Discussion with Reviewers

**A. Jakubowicz:** The authors say that the above a certain threshold value of defect density an inversion of conductivity type may occur. Based on this assumption, the authors employ a Schottky contact-like approach to interpret their EBIC results. They report inversion at the surface and the appearance of a buried space charge region related to Au-decorated misfit dislocations in the Au-decorated samples after annealing them above 1000°C. the authors give an interpretation of the temperature dependences of the EBIC signal. In this interpretation, they do not consider the temperature dependence of recombination at dislocations. How can the authors be sure that their EBIC temperature behavior is not affected by the temperature behavior of recombination at these misfit dislocations? A lot of theoretical and experimental work has been done on EBIC temperature dependences measured at extended defects which were considered as recombination sites. These temperature dependences turned out to be quite complex.

Both increase and decrease of EBIC recombination contrast versus temperature have been reported. For example, an increase of EBIC contrast with temperature at Ni and Cu precipitates was reported very recently by S. Kusanagi, T. Sekiguchi and K. Sumino (*Appl. Phys. Lett.* (1992) **61**, 792). The same authors report a decrease of EBIC contrast as a function of temperature between 100 and 300K, measured at dislocations. Any comments on this?

**Authors:** Yes, we are aware of these observations, however, the inversion effect observed in our work can not be explained by the temperature dependence of recombination activity only. In the Sumino work or a recent paper by M. Kittler, W. Seifert and Z. J. Radzimski (*Appl. Phys. Lett.* **62**(20), 1993), the recombination, i.e. decrease of the EBIC signal in the presence of electrically active defects is discussed. Our study shows that the signal outside the Schottky contact is higher in comparison with the signal measured on the Schottky and this relation reverses when the temperature is decreased. It is important to add that we are illustrating the defect inversion effect using the surface inversion only. The temperature dependence of inversion at the dislocations has not been yet studied. Additional work is in progress.

**A. Jakubowicz:** How feasible is the practical use of inversion layers fabricated by introducing extended defects in combination with gettering effects?

**Authors:** The prospect for applications of intentionally decorated misfit dislocations depends on how precisely one can control the electrical activity of these defect complexes and how stable this activity would be. A very encouraging fact is that the depth and density of misfit dislocations can be precisely controlled at this stage. Misfit dislocation decorated with gold have already been used in power switching diodes to increase their switching speed (A. S. M. Salih, (1991) *MRS Symp. Proc.* **221**, 375). In this case the misfit dislocations were located within the space charge region and their gettering and recombination properties were used.

**A. Jakubowicz:** Have the authors observed any effect of their high temperature treatments on shallow dopants, in particular in close vicinity to extended defects, where interactions with dislocations and precipitates is possible.

**Authors:** This issue was not directly addressed in this work. Our recent unpublished observations show that the temperature dependence of electrical activity for gold decorated dislocations is similar to that of shallow level defect. The possible explanation could be that both shallow and deep level defects take part in the recombination process, however the temperature dependence will be dominated by shallow defects. The shallow levels could be associated with dislocations or dopants while deep levels are Au defects in this case.

**M. Kittler:** It was noted in the literature that bevel preparation using a glass plate may invert the type of conductivity of Si (see e.g. M. Kittler and K. W. Schröter, *Physica. Stat. Sol.* (1983) **A 77**, 139). Further, chemico-mechanical polishing was observed to activate extended defects, i.e. to make defect visible in EBIC, being invisible before polishing (see e.g. M. Kittler and W. Seifert, *Proc. MRS Meeting "Defect Engineering"*, San

Francisco, May 1992). How did you prepare the bevels shown in Figs. 5 and 6, and, do you expect an influence of the preparation (may be similar to the above mentioned effects) on the contrast observed in your work?

**Authors:** The beveled samples were polished using glass plate and colloidal silica SYTON HT50 by Monsanto. So far, in our work we have not observed the type of conductivity inversion due to polishing. If such effect would occur we should observe an extended EBIC contrast on the samples annealed at lower temperatures too. We agree, that a chemico-mechanical polishing could influence the activity of misfit dislocations or other structural defects, especially when a heat treatment follows the polishing process.

**M. Kittler:** In your samples networks of buried misfit dislocations are formed at two interface planes, at the lower plane between Si buffer and Si(Ge) layer and at the upper plane between Si(Ge) layer and capping layer. Are the observed EBIC effects of misfit dislocations related to dislocations of both interfaces or not? In the case that only one interface network dominates - as it seems using the observations shown for the bevels in Fig. 5 and 6 - please comment this finding.

**Authors:** In our structures we always have two interfacial planes of misfit dislocations if a Si capping layer is grown on the Si(Ge) layer. Due to a gradient of Ge concentration in the epi-reactor the lower interface always has a higher density of dislocations than the upper interface. Although we did not observe a significant difference in decoration between lower and upper networks, the inversion effect is more likely to occur at the denser lower interface. This would explain the enhanced contrast at the bottom interface.

**M. Kittler:** In the discussion of Au decorated samples you state a typical acceptor trap for Au has an energy level 0.1 above the intrinsic level, i.e.  $E^{a_T} = E_i + 0.1$  eV. However, using well accepted literature data for Au levels in Si one gets an acceptor level  $E^{a_T} = E_C - 0.54$  eV and a donor level  $E^{d_T} = E_V + 0.33$  eV. (see e.g. N. G. Einspruch, G. B. Larrabe, VLSI Electronics, Microstructure Science, vol 6. (Materials and Process Characterization) Academic Press (1983), Chapter 1, 1-73). Using as reference level  $E_i = E_C - 1/2 E_{gap} = E_C + 0.56$  eV one gets the gold acceptor level near mid-gap at  $E^{a_T} = E_i + 0.02$  eV and not at  $E_i + 0.1$  eV. Please comment on this discrepancy.

**Authors:** Yes, we agree with this comment. The 0.1 eV level used in this paper was used only to qualitatively illustrate the temperature behavior of deep level defect. In a quantitative analysis the 0.02 level should be used. However, one should remember that, depending on the annealing temperature a range of levels are indicated for gold decoration.